Pulse design for multilevel systems by utilizing Lie transforms

Yi-Hao Kang,[1,2] Ye-Hong Chen,[1,2] Zhi-Cheng Shi,[1,2] Bi-Hua Huang,[1,2] Jie Song,[3] and Yan Xia[1,2,*]

[1]*Department of Physics, Fuzhou University, Fuzhou 350116, China*

[2]*Fujian Key Laboratory of Quantum Information and Quantum Optics, Fuzhou University, Fuzhou 350116, China*

[3]*Department of Physics, Harbin Institute of Technology, Harbin 150001, China*

(Received 20 October 2017; revised manuscript received 4 March 2018; published 19 March 2018)

We put forward a scheme to design pulses to manipulate multilevel systems with Lie transforms. A formula to reverse construct a control Hamiltonian is given and is applied in pulse design in the three- and four-level systems as examples. To demonstrate the validity of the scheme, we perform numerical simulations, which show the population transfers for cascaded three-level and N-type four-level Rydberg atoms can be completed successfully with high fidelities. Therefore, the scheme may benefit quantum information tasks based on multilevel systems.

DOI: 10.1103/PhysRevA.97.033407

I. INTRODUCTION

Controlling quantum systems with electromagnetic pulses is a critical element permeating through different research fields in quantum information processing (QIP) [1–3]. Thus, designing realizable pulses to achieve quantum information tasks accurately and robustly has been a very hot topic in recent decades. So far, many methods, such as composite pulse sequences [4,5], adiabatic passages [6–10], quantum optimal control [11–18], etc., have been presented to execute the pulse design. Among these methods [4–18], adiabatic passage [6–10] is attractive because of its robustness characteristic. This robustness comes from the fact that the system will evolve along the eigenstates of the Hamiltonian from an initial state to a target state when the control parameters vary slowly. Although it has the desirable advantage of robustness, adiabatic passage also has the undesirable weakness of long evolution time. To overcome this shortcoming, recently, a series of works named shortcut to adiabaticity (STA) [19–52] has been put forward. The aim of STA is to accelerate adiabatic passage and provide us with ways to handle quantum information tasks in a fast and robust manner. To date, STA has become even more mature and has provided us many approaches to designing pulses for fast and robust control of quantum systems.

To construct the STA well, it is beneficial to analyze the dynamic symmetry of the system because by doing so, we can easily find the parameters that control the evolution and there is no need to modify the structure of the Hamiltonian of the system. Moreover, useful results found by analyzing the dynamic symmetry of a system can be generalized to many other systems with similar structures through transformations and parametric substitutions. Since many physical systems can be depicted by a multilevel model, it is rather important to analyze the dynamic symmetry of a multilevel structure. For multilevel systems, Lie algebra and Lie transforms are deemed very powerful tools to investigate dynamic symmetry and construct the STA [50–52]. Previous schemes [50–52] have provided two different perspectives. One is to search for dynamics invariants within a Lie algebra where the Hamiltonian of the system is the superposition of several generators [50,51]. The other is using Lie transforms to find a suitable evolution path [52]. Their common feature is to describe the Hamiltonian with generators of a Lie algebra.

In this paper, inspired by earlier schemes [50–52], we propose an alternative scheme to design pulses to manipulate multilevel systems via a sequence of Lie transforms. For the sake of clarity, we show how to design pulses with Lie transforms in three- and four-level systems. Moreover, we numerically simulate population transfers of cascaded three-level and N-type four-level Rydberg atoms to check the validity of the scheme for the three- and four-level systems. The results show the population transfers can be accomplished with high accuracy. Furthermore, by suitably choosing the function for the control parameters, the pulses designed by the scheme can be smooth without any singularity. Since the formula given in the scheme can be used to construct a Hamiltonian for different multilevel systems, it may be a choice for manipulating multilevel systems in different types of quantum information processing.

II. PULSE DESIGN WITH LIE TRANSFORMS

Now, we introduce the method designing pulses with Lie transforms. Assume the Hamiltonian of a system can be written as

$$H(t)=\sum_{j=1}^{N}\lambda_j(t)A_j, \tag{1}$$

with time-dependent parameters $\lambda_j(t)$. In addition, $\{A_j\}$ is a set of Hermitian generators spanning a Lie algebra. Considering $\{A_j\}$ to be the basis for an N-dimensional Hilbert space $\mathcal{A}$, the Hamiltonian $H(t)$ can be described by a vector in $\mathcal{A}$ as

$$H(t)=\begin{bmatrix}\lambda_1(t)\\ \lambda_2(t)\\ \cdots\\ \lambda_N(t)\end{bmatrix}. \tag{2}$$

*xia-208@163.com

Next, we define a set of Lie transforms $\{\mathscr{L}_j\}$. The function of $\mathscr{L}_j$ on an arbitrary vector $A \in \mathcal{A}$ can be calculated by

$$\mathscr{L}_j(A) = e^{i\theta_j(t)A_j} A e^{-i\theta_j(t)A_j}, \tag{3}$$

with $\theta_j(t)$ being a designable time-dependent parameter. It is obvious that $\mathscr{L}_j$ can be described by an $N \times N$ matrix in $\mathcal{A}$. On the other hand, we define a set of picture transforms $\{\mathscr{P}_j\}$ based on Lie transforms $\{\mathscr{L}_j\}$. The function of $\mathscr{P}_j$ on Hamiltonian $H(t)$ is

$$\begin{aligned}\mathscr{P}_j(H) &= e^{i\theta_j(t)A_j} H(t) e^{-i\theta_j(t)A_j} - i e^{i\theta_j(t)A_j} \frac{d}{dt}(e^{-i\theta_j(t)A_j}) \\ &= \mathscr{L}_j(H) - \dot{\theta}_j(t) A_j. \end{aligned} \tag{4}$$

Now, we consider the compound picture transform

$$\mathscr{P}_N \circ \cdots \circ \mathscr{P}_2 \circ \mathscr{P}_1, \tag{5}$$

where the symbol $\circ$ denotes the compound of two transforms; we obtain the equation

$$\begin{aligned}&\mathscr{P}_N \circ \cdots \circ \mathscr{P}_2 \circ \mathscr{P}_1(H) \\ &= \mathscr{L}_N \circ \cdots \circ \mathscr{L}_2 \circ \mathscr{L}_1(H) \\ &\quad - \dot{\theta}_1(t)\mathscr{L}_N \circ \cdots \circ \mathscr{L}_3 \circ \mathscr{L}_2(A_1) \\ &\quad - \dot{\theta}_2(t)\mathscr{L}_N \circ \cdots \circ \mathscr{L}_4 \circ \mathscr{L}_3(A_2) \\ &\quad - \cdots \\ &\quad - \dot{\theta}_{N-2}(t)\mathscr{L}_N \circ \mathscr{L}_{N-1}(A_{N-2}) \\ &\quad - \dot{\theta}_{N-1}(t)\mathscr{L}_N(A_{N-1}) - \dot{\theta}_N(t) A_N. \end{aligned} \tag{6}$$

Equation (6) offers us N parameters $\{\theta_1,\theta_2,\ldots,\theta_N\}$, which also provides the possibility to reverse design N control parameters $\{\lambda_1,\lambda_2,\ldots,\lambda_N\}$. By setting $\mathscr{P}_N \circ \cdots \circ \mathscr{P}_2 \circ \mathscr{P}_1(H) = 0$, it is not difficult to prove the function of the compound picture transform in Eq. (5) is the same as the picture transform defined by the evolution operator,

$$\mathscr{P}_U(H) = U^\dagger(t) H(t) U(t) - i U^\dagger(t)\dot{U}(t) = 0, \tag{7}$$

where the result $H(t) = i\dot{U}(t)U^\dagger(t)$ is used. Thus, if the initial time is $t_i = 0$, the evolution operator of the system is

$$\begin{aligned}U(t) = &e^{-i\theta_1(t)A_1} e^{-i\theta_2(t)A_2} \cdots e^{-i\theta_N(t)A_N} \\ &\times e^{i\theta_N(0)A_N} e^{i\theta_{N-1}(0)A_{N-1}} \cdots e^{i\theta_1(0)A_1}. \end{aligned} \tag{8}$$

In this case, we obtain

$$\begin{aligned}&\mathscr{L}_N \circ \cdots \circ \mathscr{L}_2 \circ \mathscr{L}_1(H) \\ &= \dot{\theta}_1(t)\mathscr{L}_N \circ \cdots \circ \mathscr{L}_3 \circ \mathscr{L}_2(A_1) \\ &\quad + \dot{\theta}_2(t)\mathscr{L}_N \circ \cdots \circ \mathscr{L}_4 \circ \mathscr{L}_3(A_2) + \cdots \\ &\quad + \dot{\theta}_{N-2}(t)\mathscr{L}_N \circ \mathscr{L}_{N-1}(A_{N-2}) \\ &\quad + \dot{\theta}_{N-1}(t)\mathscr{L}_N(A_{N-1}) + \dot{\theta}_N(t) A_N. \end{aligned} \tag{9}$$

Generally, when $\{\lambda_j(t)\}$ are given, $\{\theta_j(t)\}$ can be solved from the N linear differential equations in Eq. (9), thus revealing the evolution operator of the system. However, obtaining analytic solutions from the differential equations in Eq. (9) is very difficult. Therefore, rather than solving $\{\theta_j(t)\}$ from known $\{\lambda_j(t)\}$, we can exploit $\{\theta_j(t)\}$ as a control parameter and reverse design $\{\lambda_j(t)\}$. We should notice that some parameters in $\{\lambda_j(t)\}$ are required to be zero according to the Hamiltonian of the specific system we investigate. Thus, the number of independent control parameters in $\{\theta_j(t)\}$ should be less than N. In this case, we can obtain constraint relations among $\{\theta_j(t)\}$ from Eq. (9).

III. APPLICATIONS IN MULTILEVEL SYSTEMS

To make the procedure of pulse design more clear, we apply the scheme to three-level and four-level systems in the following.

A. Three-level system

1. Resonant case

Considering a three-level system with the Hamiltonian

$$H_3(t) = \begin{bmatrix} 0 & \tilde{\Omega}_1(t) & 0 \\ \tilde{\Omega}_1(t) & 0 & \tilde{\Omega}_2(t) \\ 0 & \tilde{\Omega}_2(t) & 0 \end{bmatrix}, \tag{10}$$

it can be rewritten as

$$H_3(t) = \tilde{\Omega}_1(t)\tilde{A}_1 + \tilde{\Omega}_2(t)\tilde{A}_2 + 0\tilde{A}_3, \tag{11}$$

with

$$\begin{aligned}\tilde{A}_1 &= \begin{bmatrix} 0 & 1 & 0 \\ 1 & 0 & 0 \\ 0 & 0 & 0 \end{bmatrix}, \\ \tilde{A}_2 &= \begin{bmatrix} 0 & 0 & 0 \\ 0 & 0 & 1 \\ 0 & 1 & 0 \end{bmatrix}, \\ \tilde{A}_3 &= \begin{bmatrix} 0 & 0 & -i \\ 0 & 0 & 0 \\ i & 0 & 0 \end{bmatrix}. \end{aligned} \tag{12}$$

The commutation relations between each pair of $\{\tilde{A}_1,\tilde{A}_2,\tilde{A}_3\}$ are

$$[\tilde{A}_1,\tilde{A}_2] = i\tilde{A}_3,\ [\tilde{A}_2,\tilde{A}_3] = i\tilde{A}_1,\ [\tilde{A}_3,\tilde{A}_1] = i\tilde{A}_2. \tag{13}$$

$\{\tilde{A}_1,\tilde{A}_2,\tilde{A}_3\}$ span a three-dimensional Lie algebra. In the basis $\{\tilde{A}_1,\tilde{A}_2,\tilde{A}_3\}$, the matrices of Lie transforms $\{\tilde{\mathscr{L}}_k\}$ defined by $\{\tilde{A}_k\}$ $(k = 1,2,3)$ are

$$\begin{aligned}\tilde{\mathscr{L}}_1 &= \begin{bmatrix} 1 & 0 & 0 \\ 0 & \cos\tilde{\theta}_1 & \sin\tilde{\theta}_1 \\ 0 & -\sin\tilde{\theta}_1 & \cos\tilde{\theta}_1 \end{bmatrix}, \\ \tilde{\mathscr{L}}_2 &= \begin{bmatrix} \cos\tilde{\theta}_2 & 0 & -\sin\tilde{\theta}_2 \\ 0 & 1 & 0 \\ \sin\tilde{\theta}_2 & 0 & \cos\tilde{\theta}_2 \end{bmatrix}, \\ \tilde{\mathscr{L}}_3 &= \begin{bmatrix} \cos\tilde{\theta}_3 & \sin\tilde{\theta}_3 & 0 \\ -\sin\tilde{\theta}_3 & \cos\tilde{\theta}_3 & 0 \\ 0 & 0 & 1 \end{bmatrix}, \end{aligned} \tag{14}$$

and $H_3(t)$ can be described by

$$H_3(t) = \begin{bmatrix} \tilde{\Omega}_1(t) \\ \tilde{\Omega}_2(t) \\ 0 \end{bmatrix}. \tag{15}$$

Here the matrix form of $\tilde{\mathscr{L}}_k$ can be obtained using

$$\tilde{\mathscr{L}}_k = \sum_{j=1}^{3} \tilde{\mathscr{T}}[e^{i\tilde{\theta}_j(t)\tilde{A}_j}\tilde{A}_j e^{-i\tilde{\theta}_j(t)A_j}](\tilde{\mathscr{T}}\tilde{A}_j)^{\dagger}, \tag{16}$$

where $\tilde{\mathscr{T}}$ is an operator that transforms $\tilde{A}_j$ to a vector,

$$\tilde{\mathscr{T}}\tilde{A}_j = \delta_{j1}\begin{bmatrix}1\\0\\0\end{bmatrix} + \delta_{j2}\begin{bmatrix}0\\1\\0\end{bmatrix} + \delta_{j3}\begin{bmatrix}0\\0\\1\end{bmatrix}, \tag{17}$$

with $\delta_{jj'}$ ($j' = 1,2,3$) being the Kronecker delta. By using Eq. (9), we obtain

$$\begin{aligned}&\tilde{\mathscr{L}}_3 \circ \tilde{\mathscr{L}}_2 \circ \tilde{\mathscr{L}}_1(H_3) = \dot{\tilde{\theta}}_1\tilde{\mathscr{L}}_3 \circ \tilde{\mathscr{L}}_2(\tilde{A}_1) + \dot{\tilde{\theta}}_2\tilde{\mathscr{L}}_3(\tilde{A}_2) + \dot{\tilde{\theta}}_3\tilde{A}_3 \Rightarrow \\ &\begin{bmatrix}\tilde{\Omega}_1\cos\tilde{\theta}_2\cos\tilde{\theta}_3 + \tilde{\Omega}_2(\sin\tilde{\theta}_1\sin\tilde{\theta}_2\cos\tilde{\theta}_3 + \cos\tilde{\theta}_1\sin\tilde{\theta}_3)\\ -\tilde{\Omega}_1\cos\tilde{\theta}_2\sin\tilde{\theta}_3 - \tilde{\Omega}_2(\sin\tilde{\theta}_1\sin\tilde{\theta}_2\sin\tilde{\theta}_3 - \cos\tilde{\theta}_1\cos\tilde{\theta}_3)\\ \tilde{\Omega}_1\sin\tilde{\theta}_2 - \tilde{\Omega}_2\sin\tilde{\theta}_1\cos\tilde{\theta}_2\end{bmatrix} = \begin{bmatrix}\dot{\tilde{\theta}}_1\cos\tilde{\theta}_2\cos\tilde{\theta}_3 + \dot{\tilde{\theta}}_2\sin\tilde{\theta}_3\\ -\dot{\tilde{\theta}}_1\cos\tilde{\theta}_2\sin\tilde{\theta}_3 + \dot{\tilde{\theta}}_2\cos\tilde{\theta}_3\\ \dot{\tilde{\theta}}_1\sin\tilde{\theta}_2 + \dot{\tilde{\theta}}_3\end{bmatrix}.\end{aligned} \tag{18}$$

With Eq. (18), $\tilde{\Omega}_1(t)$ and $\tilde{\Omega}_2(t)$ can be reverse solved as

$$\begin{aligned}\tilde{\Omega}_1(t) &= \dot{\tilde{\theta}}_1 - \dot{\tilde{\theta}}_2\tan\tilde{\theta}_1\tan\tilde{\theta}_2,\\ \tilde{\Omega}_2(t) &= \dot{\tilde{\theta}}_2/\cos\tilde{\theta}_1,\end{aligned} \tag{19}$$

with a constraint equation for $\tilde{\theta}_3$,

$$\dot{\tilde{\theta}}_3 = -\dot{\tilde{\theta}}_2\tan\tilde{\theta}_1/\cos\tilde{\theta}_2. \tag{20}$$

Moreover, the evolution operator can be derived from Eq. (8) as

$$U_3(t) = \begin{bmatrix}\cos\tilde{\theta}_1\cos\tilde{\theta}_3 - \sin\tilde{\theta}_1\sin\tilde{\theta}_2\sin\tilde{\theta}_3 & -i\sin\tilde{\theta}_1\cos\tilde{\theta}_2 & -\cos\tilde{\theta}_1\sin\tilde{\theta}_3 - \sin\tilde{\theta}_1\sin\tilde{\theta}_2\cos\tilde{\theta}_3\\ -i(\sin\tilde{\theta}_1\cos\tilde{\theta}_3 + \cos\tilde{\theta}_1\sin\tilde{\theta}_2\sin\tilde{\theta}_3) & \cos\tilde{\theta}_1\cos\tilde{\theta}_2 & i(\sin\tilde{\theta}_1\sin\tilde{\theta}_3 - \cos\tilde{\theta}_1\sin\tilde{\theta}_2\cos\tilde{\theta}_3)\\ \cos\tilde{\theta}_2\sin\tilde{\theta}_3 & -i\sin\tilde{\theta}_2 & \cos\tilde{\theta}_2\cos\tilde{\theta}_3\end{bmatrix} \tag{21}$$

if $\tilde{\theta}_1(0) = \tilde{\theta}_2(0) = \tilde{\theta}_3(0) = 0$.

2. Off-resonant case

In the above discussions, we considered the pulse design of a three-level system in the resonant case. Now, let us briefly consider the pulse design of a three-level system in the off-resonant case. Consider a three-level system with the Hamiltonian

$$\grave{H}_3(t) = \begin{bmatrix}\Delta_1(t) & \grave{\Omega}_1^*(t) & 0\\ \grave{\Omega}_1(t) & \Delta_2(t) & \grave{\Omega}_2(t)\\ 0 & \grave{\Omega}_2^*(t) & \Delta_3(t)\end{bmatrix}. \tag{22}$$

$\grave{H}_3(t)$ can be expanded by

$$\grave{H}_3(t) = \grave{\Omega}_{1r}(t)\grave{A}_2 + \grave{\Omega}_{2r}(t)\grave{A}_3 + \grave{\Omega}_{1i}(t)\grave{A}_5 + \grave{\Omega}_{2i}(t)\grave{A}_6 + \delta_1(t)\grave{A}_7 + \delta_2(t)\grave{A}_8 + \delta_3(t)I_3, \tag{23}$$

where I_3 is the identity operator of the three-level system and $\grave{\Omega}_{1r}(t)$ and $\grave{\Omega}_{1i}(t)$ [$\grave{\Omega}_{2r}(t)$ and $\grave{\Omega}_{2i}(t)$] are real part and imaginary parts of $\grave{\Omega}_1(t)$ ($\grave{\Omega}_2(t)$), respectively. The parameters $\delta_1(t)$, $\delta_2(t)$, and $\delta_3(t)$ read

$$\begin{aligned}\delta_1(t) &= [2\Delta_1(t) - \Delta_2(t) - \Delta_3(t)]/3,\\ \delta_2(t) &= [-\Delta_1(t) + 2\Delta_2(t) - \Delta_3(t)]/3,\\ \delta_3(t) &= [\Delta_1(t) + \Delta_2(t) + \Delta_3(t)]/3,\end{aligned} \tag{24}$$

respectively. Also, $\{\grave{A}_J | J = 1,2,\ldots,8\}$ are listed in Appendix A. By neglecting the global phase

$$\Theta(t) = -\int_0^t \delta_3(t')dt', \tag{25}$$

we omit the term $\delta_3(t)I_3$ in Eq. (23). With Eqs. (8) and (9), we can derive (see Appendix A for details)

$$\begin{aligned}
\grave{\Omega}_{1r}(t) &= \dot{\grave{\theta}}_5 \sin\grave{\theta}_1 + \dot{\grave{\theta}}_6 \cos\grave{\theta}_1 \sin\grave{\theta}_5,\\
\grave{\Omega}_{1i}(t) &= \frac{3\dot{\grave{\theta}}_7}{4}\sin\grave{\theta}_1 \sin 2\grave{\theta}_5 + \frac{\dot{\grave{\theta}}_7 + 2\dot{\grave{\theta}}_8}{2}\sin\grave{\theta}_5(\cos\grave{\theta}_1 \sin 2\grave{\theta}_6 - \sin\grave{\theta}_1 \cos\grave{\theta}_5 \cos 2\grave{\theta}_6),\\
\grave{\Omega}_{2r}(t) &= \frac{3\dot{\grave{\theta}}_7}{4}\cos\grave{\theta}_1 \sin 2\grave{\theta}_5 - \frac{\dot{\grave{\theta}}_7 + 2\dot{\grave{\theta}}_8}{2}\sin\grave{\theta}_5(\sin\grave{\theta}_1 \sin 2\grave{\theta}_6 + \cos\grave{\theta}_1 \cos\grave{\theta}_5 \cos 2\grave{\theta}_6),\\
\grave{\Omega}_{2i}(t) &= -\dot{\grave{\theta}}_5 \cos\grave{\theta}_1 + \dot{\grave{\theta}}_6 \sin\grave{\theta}_1 \sin\grave{\theta}_5,\\
\delta_1(t) &= -\frac{\dot{\grave{\theta}}_7 + 2\dot{\grave{\theta}}_8}{8}[4\sin 2\grave{\theta}_1 \cos\grave{\theta}_5 \sin 2\grave{\theta}_6 + \cos 2\grave{\theta}_6(-2\sin^2\grave{\theta}_1 \cos 2\grave{\theta}_5 + 3\cos 2\grave{\theta}_1 + 1)]\\
&\quad - \frac{\dot{\grave{\theta}}_7}{8}(6\sin^2\grave{\theta}_1 \cos 2\grave{\theta}_5 + 3\cos 2\grave{\theta}_1 + 1),\\
\delta_2(t) &= \frac{\dot{\grave{\theta}}_7 + 2\dot{\grave{\theta}}_8}{2}\sin^2\grave{\theta}_5 \cos 2\grave{\theta}_6 + \frac{\dot{\grave{\theta}}_7}{4}(1 + 3\cos 2\grave{\theta}_5),
\end{aligned} \tag{26}$$

and the constraint equations

$$\begin{aligned}
\dot{\grave{\theta}}_1 &= \dot{\grave{\theta}}_6 \cos\grave{\theta}_5,\\
\dot{\grave{\theta}}_8 &= -\dot{\grave{\theta}}_7 \frac{\chi(t) + 6\sin 2\grave{\theta}_1 \sin^2\grave{\theta}_5}{2\chi(t)},
\end{aligned} \tag{27}$$

with

$$\chi(t) = \sin 2\grave{\theta}_1(3 + \cos 2\grave{\theta}_5)\cos 2\grave{\theta}_6 - 4\cos 2\grave{\theta}_1 \cos\grave{\theta}_5 \sin 2\grave{\theta}_6. \tag{28}$$

Assuming $\grave{\theta}_{j'}(0) = 0$ ($j' = 1,5,6,7,8$), according to Eq. (8), the evolution can be derived as

$$\grave{U}_3(t) = \begin{bmatrix} -\sin\grave{\theta}_1 \sin\grave{\theta}_5 & \cos\grave{\theta}_1 \sin\grave{\theta}_6 - \cos\grave{\theta}_5 \cos\grave{\theta}_6 \sin\grave{\theta}_1 & -\cos\grave{\theta}_1 \cos\grave{\theta}_6 + \cos\grave{\theta}_5 \sin\grave{\theta}_1 \sin\grave{\theta}_6 \\ -i\cos\grave{\theta}_5 & i\cos\grave{\theta}_6 \sin\grave{\theta}_5 & i\sin\grave{\theta}_5 \sin\grave{\theta}_6 \\ -i\cos\grave{\theta}_1 \sin\grave{\theta}_5 & -i\cos\grave{\theta}_1 \cos\grave{\theta}_5 \cos\grave{\theta}_6 + \sin\grave{\theta}_1 \sin\grave{\theta}_6 & i\cos\grave{\theta}_6 \sin\grave{\theta}_1 - \cos\grave{\theta}_1 \cos\grave{\theta}_5 \sin\grave{\theta}_6 \end{bmatrix} \grave{U}_t \grave{U}_0, \tag{29}$$

with

$$\grave{U}_0 = \begin{bmatrix} 0 & i & 0 \\ 0 & 0 & i \\ -1 & 0 & 0 \end{bmatrix}, \grave{U}_t = \begin{bmatrix} e^{-i\dot{\grave{\theta}}_7} & 0 & 0 \\ 0 & e^{-i\dot{\grave{\theta}}_8} & 0 \\ 0 & 0 & e^{i(\dot{\grave{\theta}}_7 + \dot{\grave{\theta}}_8)} \end{bmatrix}. \tag{30}$$

B. Four-level system

Consider a four-level system with the Hamiltonian

$$H_4(t) = \begin{bmatrix} 0 & \overline{\Omega}_1(t) & 0 & 0 \\ \overline{\Omega}_1(t) & 0 & \overline{\Omega}_2(t) & 0 \\ 0 & \overline{\Omega}_2(t) & 0 & \overline{\Omega}_3(t) \\ 0 & 0 & \overline{\Omega}_3(t) & 0 \end{bmatrix}. \tag{31}$$

$H_4(t)$ can be expanded by

$$H_4(t) = \overline{\Omega}_1(t)\overline{A}_1 + \overline{\Omega}_2(t)\overline{A}_2 + \overline{\Omega}_3(t)\overline{A}_3 + 0(\overline{A}_4 + \overline{A}_5 + \overline{A}_6), \tag{32}$$

where $\overline{A}_l$ ($l = 0,1,2,\ldots,6$) are shown in Appendix B. By using Eqs. (8) and (9), we can derive (see Appendix B for details)

$$\begin{aligned}
\overline{\Omega}_1(t) &= \dot{\overline{\theta}}_1 + \dot{\overline{\theta}}_5 \sin\overline{\theta}_3 \cos\overline{\theta}_4 + \dot{\overline{\theta}}_6 \cos\overline{\theta}_3 \sin\overline{\theta}_4,\\
\overline{\Omega}_2(t) &= \dot{\overline{\theta}}_3 \cos\overline{\theta}_1 \cos\overline{\theta}_2 + \dot{\overline{\theta}}_4 \sin\overline{\theta}_1 \sin\overline{\theta}_2 - \dot{\overline{\theta}}_5(\sin\overline{\theta}_1 \cos\overline{\theta}_2 \cos\overline{\theta}_3 \cos\overline{\theta}_4 + \cos\overline{\theta}_1 \sin\overline{\theta}_2 \sin\overline{\theta}_3 \sin\overline{\theta}_4)\\
&\quad + \dot{\overline{\theta}}_6(\cos\overline{\theta}_1 \sin\overline{\theta}_2 \cos\overline{\theta}_3 \cos\overline{\theta}_4 + \sin\overline{\theta}_1 \cos\overline{\theta}_2 \sin\overline{\theta}_3 \sin\overline{\theta}_4),\\
\overline{\Omega}_3(t) &= \dot{\overline{\theta}}_2 - \dot{\overline{\theta}}_5 \cos\overline{\theta}_3 \sin\overline{\theta}_4 - \dot{\overline{\theta}}_6 \sin\overline{\theta}_3 \cos\overline{\theta}_4,
\end{aligned} \tag{33}$$

and the constraint equations

$$\begin{aligned}\dot{\overline{\theta}}_4 &= \dot{\overline{\theta}}_3 \tan\overline{\theta}_1 \tan\overline{\theta}_2,\\ \dot{\overline{\theta}}_5 &= \frac{2\dot{\overline{\theta}}_3(\sin\overline{\theta}_3 \sin\overline{\theta}_4 \tan\overline{\theta}_2 - \cos\overline{\theta}_3 \cos\overline{\theta}_4 \tan\overline{\theta}_1)}{\cos 2\overline{\theta}_3 + \cos 2\overline{\theta}_4},\\ \dot{\overline{\theta}}_6 &= \frac{2\dot{\overline{\theta}}_3(\cos\overline{\theta}_3 \cos\overline{\theta}_4 \tan\overline{\theta}_2 - \sin\overline{\theta}_3 \sin\overline{\theta}_4 \tan\overline{\theta}_1)}{\cos 2\overline{\theta}_3 + \cos 2\overline{\theta}_4}.\end{aligned} \tag{34}$$

Further, when $\overline{\theta}_l(0) = 0$ ($l = 0,1,2,\ldots,6$), the evolution operator reads

$$U_4(t) = \begin{bmatrix} \cos\overline{\theta}_1\cos\overline{\theta}_4\cos\overline{\theta}_5 - \sin\overline{\theta}_1\sin\overline{\theta}_3\sin\overline{\theta}_5 & -i(\cos\overline{\theta}_3\cos\overline{\theta}_6\sin\overline{\theta}_1 + \cos\overline{\theta}_1\sin\overline{\theta}_4\sin\overline{\theta}_6) \\ -i(\cos\overline{\theta}_4\cos\overline{\theta}_5\sin\overline{\theta}_1 + \cos\overline{\theta}_1\sin\overline{\theta}_3\sin\overline{\theta}_5) & \cos\overline{\theta}_1\cos\overline{\theta}_3\cos\overline{\theta}_6 - \sin\overline{\theta}_1\sin\overline{\theta}_4\sin\overline{\theta}_6 \\ \cos\overline{\theta}_2\cos\overline{\theta}_3\sin\overline{\theta}_5 - \cos\overline{\theta}_5\sin\overline{\theta}_2\sin\overline{\theta}_4 & -i(\cos\overline{\theta}_2\cos\overline{\theta}_6\sin\overline{\theta}_3 + \cos\overline{\theta}_4\sin\overline{\theta}_2\sin\overline{\theta}_6) \\ -i(\cos\overline{\theta}_2\cos\overline{\theta}_5\sin\overline{\theta}_4 + \cos\overline{\theta}_3\sin\overline{\theta}_2\sin\overline{\theta}_5) & \cos\overline{\theta}_2\cos\overline{\theta}_4\sin\overline{\theta}_6 - \cos\overline{\theta}_6\sin\overline{\theta}_2\sin\overline{\theta}_3 \end{bmatrix}$$

$$\begin{bmatrix} -\cos\overline{\theta}_5\sin\overline{\theta}_1\sin\overline{\theta}_3 - \cos\overline{\theta}_1\cos\overline{\theta}_4\sin\overline{\theta}_5 & -i(\cos\overline{\theta}_1\cos\overline{\theta}_6\sin\overline{\theta}_4 - \cos\overline{\theta}_3\sin\overline{\theta}_1\sin\overline{\theta}_6) \\ -i(\cos\overline{\theta}_1\cos\overline{\theta}_5\sin\overline{\theta}_3 - \cos\overline{\theta}_4\sin\overline{\theta}_1\sin\overline{\theta}_5) & -\cos\overline{\theta}_6\sin\overline{\theta}_1\sin\overline{\theta}_4 - \cos\overline{\theta}_1\cos\overline{\theta}_3\sin\overline{\theta}_6 \\ \cos\overline{\theta}_2\cos\overline{\theta}_3\cos\overline{\theta}_5 + \sin\overline{\theta}_2\sin\overline{\theta}_4\sin\overline{\theta}_5 & -i(\cos\overline{\theta}_4\cos\overline{\theta}_6\sin\overline{\theta}_2 - \cos\overline{\theta}_2\sin\overline{\theta}_3\sin\overline{\theta}_6) \\ -i(\cos\overline{\theta}_3\cos\overline{\theta}_5\sin\overline{\theta}_2 - \cos\overline{\theta}_2\sin\overline{\theta}_4\sin\overline{\theta}_5) & \cos\overline{\theta}_2\cos\overline{\theta}_4\cos\overline{\theta}_6 + \sin\overline{\theta}_2\sin\overline{\theta}_3\sin\overline{\theta}_6 \end{bmatrix}. \tag{35}$$

IV. EXAMPLES: POPULATION TRANSFERS FOR CASCADED THREE-LEVEL AND *N*-TYPE FOUR-LEVEL RYDBERG ATOMS

In this section, we exploit the results shown in Sec. III to realize population transfers of cascaded three-level and N-type four-level Rydberg atoms, whose level structures are very useful in the research field of Rydberg atoms [53–57].

A. Cascaded three-level Rydberg atom

1. Resonant case

As shown in Fig. 1, we consider a cascaded three-level Rydberg atom with a ground state $|g\rangle$, an intermediate state $|e\rangle$, and a Rydberg state $|r\rangle$ [53]. In experiments, the atomic structure can be obtained by using a ^{87}Rb atom with $|g\rangle = |5s_{1/2}, F = 1, M_F = 1\rangle$, $|e\rangle = |5p_{1/2}, F = 2, M_F = 2\rangle$, and $|r\rangle = |58d_{3/2}, F = 3, M_F = 3\rangle$ [53,54]. In the basis $\{|g\rangle,|e\rangle,|r\rangle\}$, the Hamiltonian of the Rydberg atom can be described by the matrix shown in Eq. (10), with $\tilde{\Omega}_1(t)$ and $\tilde{\Omega}_2(t)$ denoting the Rabi frequencies of laser pulses driving transitions $|g\rangle \leftrightarrow |e\rangle$ and $|e\rangle \leftrightarrow |r\rangle$, respectively. Assume the Rydberg atom is initially in the state $|g\rangle$, and we want to bump it to the Rydberg state $|r\rangle$. According to the evolution operator given in Eq. (21), the evolution of the Rydberg atom can be described by

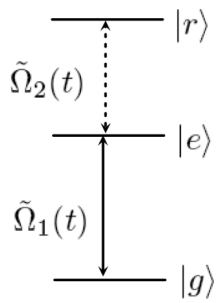

FIG. 1. The level configuration of a cascaded three-level Rydberg atom.

$$\begin{aligned}|\psi_3(t)\rangle &= U_3(t)|g\rangle\\ &= (\cos\tilde{\theta}_1\cos\tilde{\theta}_3 - \sin\tilde{\theta}_1\sin\tilde{\theta}_2\sin\tilde{\theta}_3)|g\rangle\\ &\quad - i(\sin\tilde{\theta}_1\cos\tilde{\theta}_3 + \cos\tilde{\theta}_1\sin\tilde{\theta}_2\sin\tilde{\theta}_3)|e\rangle\\ &\quad + \cos\tilde{\theta}_2\sin\tilde{\theta}_3|r\rangle.\end{aligned} \tag{36}$$

Therefore, we can choose the boundary conditions

$$\tilde{\theta}_1(T) = 0,\ \tilde{\theta}_2(T) = 0,\ \tilde{\theta}_3(T) = \pi/2, \tag{37}$$

where T is the final time. According to Eq. (37), parameters $\tilde{\theta}_1(t)$ and $\tilde{\theta}_2(t)$ can be chosen to be

$$\begin{aligned}\tilde{\theta}_1(t) &= -\Upsilon_1 \sin\left(\frac{2\pi t}{T}\right)\sin\left(\frac{\pi t}{T}\right),\\ \tilde{\theta}_2(t) &= \frac{\Upsilon_2}{2}\left[1 - \cos\left(\frac{2\pi t}{T}\right)\right],\end{aligned} \tag{38}$$

where Υ_1 and Υ_2 are two time-independent parameters controlling the maximal values of $|\tilde{\theta}_1(t)|$ and $|\tilde{\theta}_2(t)|$, respectively. According to Eqs. (20) and (37), Υ_1 and Υ_2 should be chosen to fulfill the condition

$$\tilde{\theta}_3(T) = -\int_0^T \frac{\dot{\tilde{\theta}}_2(t)\tan[\tilde{\theta}_1(t)]}{\cos[\tilde{\theta}_2(t)]}dt = \pi/2. \tag{39}$$

Considering that Eq. (39) has a singularity when $\tilde{\theta}_1 = \pi/2$ or $\tilde{\theta}_2 = \pi/2$, it is better to restrict ourselves to $\Upsilon_1 \in [0,\pi/2]$ and $\Upsilon_2 \in [0,\pi/2]$. By numerically calculating Eq. (39), the relation between Υ_1 and Υ_2 can be shown by Fig. 2. When $\Upsilon_1 < 0.5$, Υ_2 should be very close to $\pi/2$. Therefore, in Fig. 2, the range of Υ_1 is set to [0.5,1.5]. As an example, we consider $\Upsilon_1 = 1.2$ and $\Upsilon_2 = 0.8281$. The populations of $|g\rangle$, $|e\rangle$, and $|r\rangle$ versus t/T are plotted in Fig. 3(a). In addition, $\tilde{\Omega}_1(t)$ and $\tilde{\Omega}_2(t)$ versus t/T are plotted in Fig. 3(b). According to Fig. 3(a), the population transfer can be achieved at $t = T$. This shows the calculation processes of the resonant case in Sec. III A are

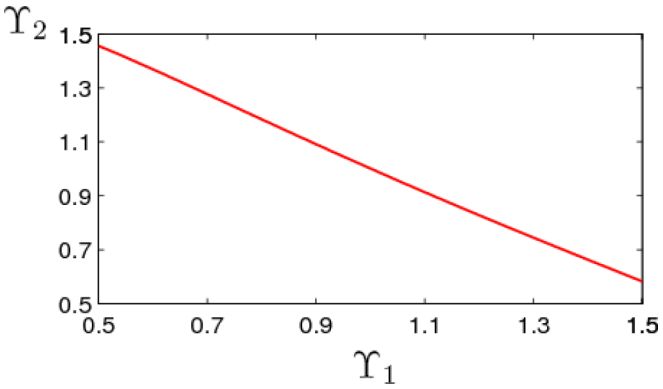

FIG. 2. The dependency relationship between Υ_1 and Υ_2.

valid. In addition, according to Fig. 3(b), we have $\tilde{\Omega}_{\max} = \max_{0\leqslant t\leqslant T}\{|\tilde{\Omega}_1(t)|,|\tilde{\Omega}_2(t)|\} = 7.54/T$.

To show the feasibility of the population transfer of the cascaded three-level Rydberg atom, we further investigate (i) curve fitting for designed pulses using pulses with an experimentally available wave shape, (ii) the performance of the population transfer when the transitions $|g\rangle \leftrightarrow |e\rangle$ and $|e\rangle \leftrightarrow |r\rangle$ are not perfectly resonantly driven by $\tilde{\Omega}_1(t)$ and $\tilde{\Omega}_2(t)$, respectively, (iii) the influence of some types of noise acting on the population transfer, and (iv) the evolution of the cascaded three-level Rydberg atom governed by the master equation when considering decoherence.

(i) In experiments, pulses with complex wave shapes are usually more difficult to obtain compared with those with simple wave shapes, such as Gaussian functions, sine functions, etc. Thus, if one can use a series of pulses with simple wave shapes to replace pulses with complex wave shapes to obtain similar outcomes, the operations may become more feasible. Here curve fitting is applied to the designed pulses $\tilde{\Omega}_1(t)$ and

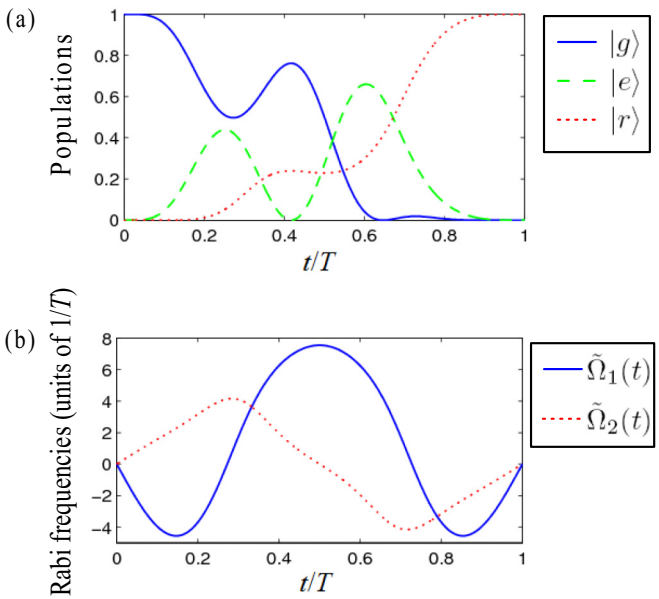

FIG. 3. (a) Populations of $|g\rangle$, $|e\rangle$, and $|r\rangle$ versus t/T. (b) $\tilde{\Omega}_1(t)$ and $\tilde{\Omega}_2(t)$ versus t/T.

TABLE I. The results of $-i[\overline{A}_l, \overline{A}_{l'}]$.

p	ζ_p	μ_p	σ_p
1	4.126	0.2875	0.1285
2	1.144	0.1214	0.0905
3	−4.126	0.7125	0.1285
4	−1.144	0.8786	0.0905
q	ξ_q	α_q	β_q
1	−4.529	11.28	0
2	7.755	6.632	−1.745
3	4.529	11.28	1.2864

$\tilde{\Omega}_2(t)$, so that they can be replaced by a series of pulses with Gaussian and sine wave shapes. The replaced pulses $\tilde{\Omega}_1'(t)$ and $\tilde{\Omega}_2'(t)$ for $\tilde{\Omega}_1(t)$ and $\tilde{\Omega}_2(t)$ can be respectively written as

$$\begin{aligned}
\tilde{\Omega}_1'(t) &= \sum_{p=1}^{4} G_p(t), \\
\tilde{\Omega}_2'(t) &= \sum_{q=1}^{3} \eta_q(t) S_q(t), \\
G_p(t) &= \frac{\zeta_p}{T} e^{-(\frac{t/T-\mu_p}{\sigma_p})^2}, \\
S_q(t) &= \frac{\xi_q}{T} \sin(\alpha_q t/T + \beta_q),
\end{aligned} \tag{40}$$

where parameters $\zeta_p, \mu_p\, \sigma_p, \xi_q, \alpha_q$, and β_q are given in Table I.

The function $\eta_q(t)$ reads

$$\eta_q(t) = \begin{cases} 1, & t \in [\tau_{q1}, \tau_{q2}], \\ 0, & \text{otherwise}, \end{cases} \tag{41}$$

with

$$\begin{aligned}
&\tau_{11} = 0, \quad \tau_{12} = 0.2785T, \quad \tau_{21} = 0.2631T, \\
&\tau_{22} = 0.7368T, \quad \tau_{31} = 0.7215T, \quad \tau_{32} = T.
\end{aligned} \tag{42}$$

Noticing $S_q(\tau_{q1}) = S_q(\tau_{q2}) = 0$, $\eta_q(t)$ lets us exploit only half a period of the sine function $S_q(t)$. To make each of the pulses $\{G_p(t), S_q(t)\}$ clear, we plot $G_p(t)$ $(p = 1,2,3,4)$ and $S_q(t)(q = 1,2,3)$ in Figs. 4(a) and 4(b), respectively. Moreover, $1 - P_r(t)$ versus t/T is plotted in Fig. 4(c), where $P_r(t) = |\langle\psi_3(t)|r\rangle|^2$ is the population of the Rydberg state $|r\rangle$. Figure 4(c) shows that by using the replaced pulses $\tilde{\Omega}_1'(t)$ and $\tilde{\Omega}_2'(t)$, we still have $1 - P_r(t) < 10^{-5}$, which means the population transfer is nearly perfect.

(ii) In the discussions above in this section, we consider transitions $|g\rangle \leftrightarrow |e\rangle$ and $|e\rangle \leftrightarrow |r\rangle$ to be resonantly driven by $\tilde{\Omega}_1(t)$ and $\tilde{\Omega}_2(t)$, respectively, while for a real experiment, there may exist some small detunings due to imperfect control of pulse frequencies. Here detuning Δ_g (Δ_r) for transitions $|g\rangle \leftrightarrow |e\rangle$ $(|e\rangle \leftrightarrow |r\rangle)$ is considered; that is, terms $\Delta_g|g\rangle\langle g|$ and $\Delta_r|r\rangle\langle r|$ are added to the Hamiltonian of the cascaded three-level Rydberg atom. By considering small detunings $|\Delta_g| \leqslant \tilde{\Omega}_{\max}/10$ and $|\Delta_r| \leqslant \tilde{\Omega}_{\max}/10$, we plot the final population

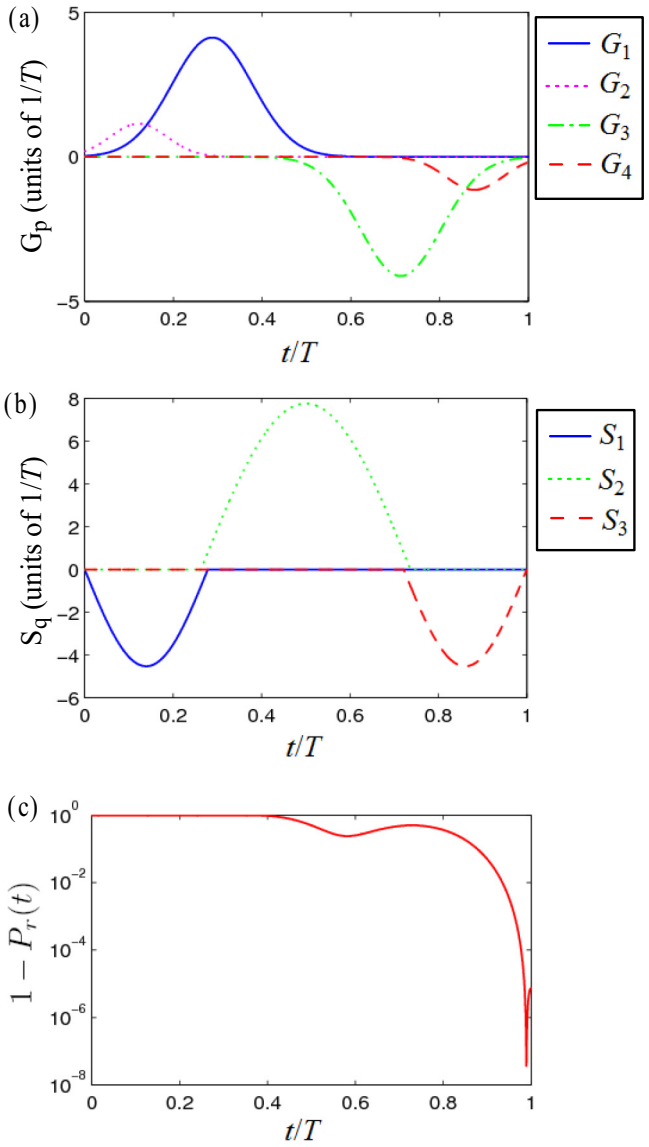

FIG. 4. (a) $G_p(t)$ $(p = 1,2,3,4)$ versus t/T. (b) $S_q(t)$ $(q = 1,2,3)$ versus t/T. (c) $1 - P_r(t)$ versus t/T.

$P_r(T) = |\langle\psi_3(T)|r\rangle|^2$ of the Rydberg state $|r\rangle$ versus $\Delta_g/\tilde{\Omega}_{\max}$ and $\Delta_r/\tilde{\Omega}_{\max}$ in Fig. 5.

According to Fig. 5, when Δ_g and Δ_r are both positive or both negative, the population transfer still maintains good performance. By taking $\Delta_g/\tilde{\Omega}_{\max} = \Delta_r/\tilde{\Omega}_{\max} = \pm 0.1$, we have $P_r(T) = 0.9931$. However, if Δ_g and Δ_r have different signs, $P_r(T)$ falls more than in the case when they have the same sign. The worst performance appears at $\Delta_g/\tilde{\Omega}_{\max} = -\Delta_r/\tilde{\Omega}_{\max} = \pm 0.1$, which gives $P_r(T) = 0.9045$. Thus, when $|\Delta_g| \leqslant \tilde{\Omega}_{\max}/10$ and $|\Delta_r| \leqslant \tilde{\Omega}_{\max}/10$, $P_r(T)$ falls less than 0.1 from 1. This shows that the population transfer remains robust against small detunings of transitions.

(iii) When using pulses to drive the transitions of an atom, there may exist a noisy component in each pulse, which disturbs the intended dynamics. Here two typical noises, the random noise of pulse amplitudes and additive white Gaussian noise (AWGN), are investigated. First, we consider the random noise of pulse amplitudes. In this case, pulses under the influence of noise can be described by

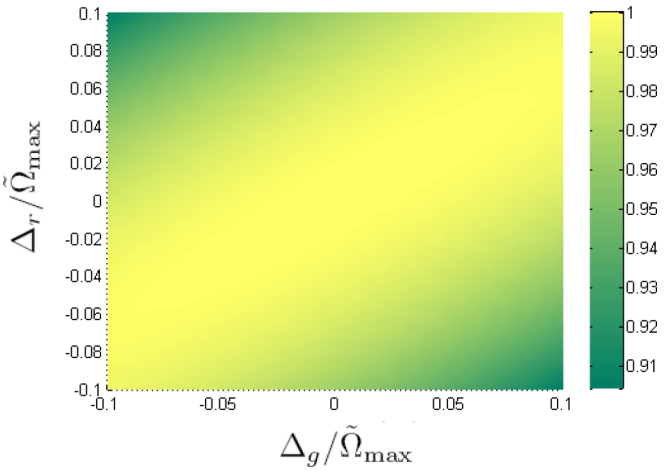

FIG. 5. Final population $P_r(T)$ of Rydberg state $|r\rangle$ versus $\Delta_g/\tilde{\Omega}_{\max}$ and $\Delta_r/\tilde{\Omega}_{\max}$.

$$\begin{aligned} \breve{\Omega}_1(t) &= [1 + R_1(t,\Gamma_1)]\tilde{\Omega}_1(t), \\ \breve{\Omega}_2(t) &= [1 + R_2(t,\Gamma_2)]\tilde{\Omega}_2(t), \end{aligned} \tag{43}$$

where $R_1(t)$ and $R_2(t)$ denote two random functions. Γ_1 (Γ_2) is the amplitude of $R_1(t)$ [$R_2(t)$]. We plot $\breve{\Omega}_1(t)$ and $\breve{\Omega}_2(t)$ versus t/T with $\Gamma_1 = \Gamma_2 = 0.1$, $\Gamma_1 = \Gamma_2 = 0.5$, and $\Gamma_1 = \Gamma_2 = 1$ in Figs. 6(a)–6(c), respectively. Also, $1 - P_r(t)$ versus t/T with $\Gamma_1 = \Gamma_2 = 0.1$, $\Gamma_1 = \Gamma_2 = 0.5$, and $\Gamma_1 = \Gamma_2 = 1$ are plotted

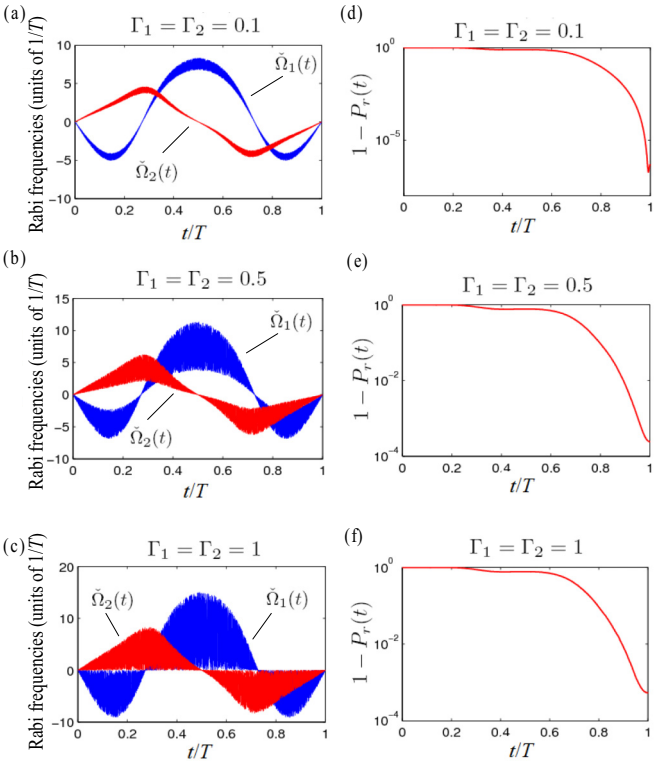

FIG. 6. $\breve{\Omega}_1(t)$ and $\breve{\Omega}_2(t)$ versus t/T with (a) $\Gamma_1 = \Gamma_2 = 0.1$, (b) $\Gamma_1 = \Gamma_2 = 0.5$, and (c) $\Gamma_1 = \Gamma_2 = 1$. Also shown is $1 - P_r(t)$ versus t/T with (d) $\Gamma_1 = \Gamma_2 = 0.1$, (e) $\Gamma_1 = \Gamma_2 = 0.5$, and (f) $\Gamma_1 = \Gamma_2 = 1$.

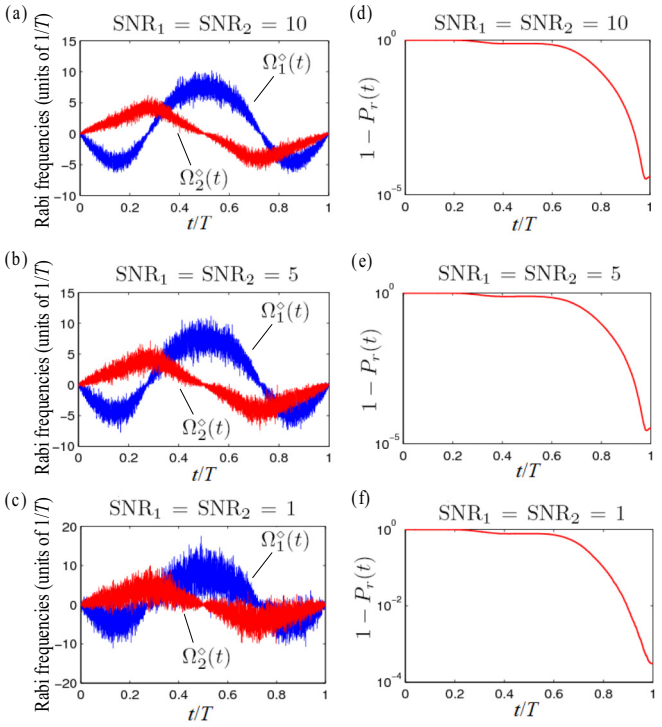

FIG. 7. $\Omega_1^\diamond(t)$ and $\Omega_2^\diamond(t)$ versus t/T with (a) $R_{SN1} = R_{SN2} = 10$, (b) $R_{SN1} = R_{SN2} = 5$, and (c) $R_{SN1} = R_{SN2} = 1$. Also shown is $1 - P_r(t)$ versus t/T with (d) $R_{SN1} = R_{SN2} = 10$, (e) $R_{SN1} = R_{SN2} = 5$, and (f) $R_{SN1} = R_{SN2} = 1$.

in Figs. 6(d)–6(f), respectively. Figures 6(d)–6(f) show that we have $1 - P_r(t) < 10^{-5}$ for $\Gamma_1 = \Gamma_2 = 0.1$ and $1 - P_r(t) < 10^{-3}$ for both $\Gamma_1 = \Gamma_2 = 0.5$ and $\Gamma_1 = \Gamma_2 = 1$. The results show that the population transfer is still effective when the random noise of the pulse amplitudes has a scale similar to that of the original pulses. Generally, the scale of noise is much smaller than the scale of the original pulses. Thus, the influences of the random noise of pulse amplitudes can be neglected for the population transfer.

Then, let us study the AWGN. In this case, pulses under the influence of noise can be described by

$$\begin{aligned}\Omega_1^\diamond(t) &= \tilde{\Omega}_1(t) + \mathrm{awgn}(\tilde{\Omega}_1(t), R_{SN1}),\\ \Omega_2^\diamond(t) &= \tilde{\Omega}_2(t) + \mathrm{awgn}(\tilde{\Omega}_2(t), R_{SN2}),\end{aligned} \tag{44}$$

where awgn is the function generating AWGN with signal-to-noise ratio R_{SN1} (R_{SN2}) for pulses $\tilde{\Omega}_1(t)$ [$\tilde{\Omega}_2(t)$]. We plot $\Omega_1^\diamond(t)$ and $\Omega_2^\diamond(t)$ versus t/T with $R_{SN1} = R_{SN2} = 10$, $R_{SN1} = R_{SN2} = 5$, and $R_{SN1} = R_{SN2} = 1$ in Figs. 7(a)–7(c), respectively. Moreover, $1 - P_r(t)$ versus t/T with $R_{SN1} = R_{SN2} = 10$, $R_{SN1} = R_{SN2} = 5$, and $R_{SN1} = R_{SN2} = 1$ are plotted in Figs. 7(d)–7(f), respectively. According to Figs. 7(d)–7(f), $1 - P_r(T) < 10^{-3}$ can be obtained with $R_{SN1} = R_{SN2} = 10$, $R_{SN1} = R_{SN2} = 5$, and $R_{SN1} = R_{SN2} = 1$. Interestingly, in the case of $R_{SN1} = R_{SN2} = 1$, where AWGN has a scale similar to that of the original pulses, the population transfer is still effective. These results indicate that the population transfer is also robust against AWGN.

(iv) Decoherence is ineluctable in real experiments. Thus, it is worth discussing the population transfer against decoherence. In experiments, as the Rydberg state $|r\rangle$ is much more stable than the intermediate state $|e\rangle$ [53,55], the main decoherence factor for the cascaded three-level Rydberg atom is the atomic spontaneous emission from the intermediate state $|e\rangle$ to the ground state $|g\rangle$. We consider the master equation

$$\begin{aligned}\dot{\rho}_3(t) = i[\rho_3(t), H_3(t)] + \gamma\big\{&S_{eg}\rho_3(t)S_{eg}^\dagger\\ &- \tfrac{1}{2}[S_{eg}^\dagger S_{eg}\rho_3(t) + \rho_3(t)S_{eg}^\dagger S_{eg}]\big\},\end{aligned} \tag{45}$$

where $\rho_3(t)$ is the density operator of the cascaded three-level Rydberg atom, γ is the spontaneous emissions rate of the decay path $|e\rangle \to |g\rangle$, and S_{eg} denotes $|g\rangle\langle e|$. The final population $P_r(T) = \langle r|\rho_3(T)|r\rangle$ of the Rydberg state $|r\rangle$ versus $\gamma/\tilde{\Omega}_{\max}$ is plotted in Fig. 8. According to Fig. 8, $P_r(T)$ decreases nearly linearly from 1 to 0.9784 when κ increases from 0 to $0.05\tilde{\Omega}_{\max}$. Consider a set of experimental parameters [53,57] $\tilde{\Omega}_{\max} = 2\pi \times 60$ MHz, $\gamma = 2\pi \times 3$ MHz, where we have the ratio $\gamma/\tilde{\Omega}_{\max} = 0.05$; the final population $P_r(T)$ of the Rydberg state $|r\rangle$ is 0.9784. The results given above show the population transfer of the cascaded three-level Rydberg atom with the pulses designed by the current scheme remains robust against atomic spontaneous emission from $|e\rangle$ to $|g\rangle$.

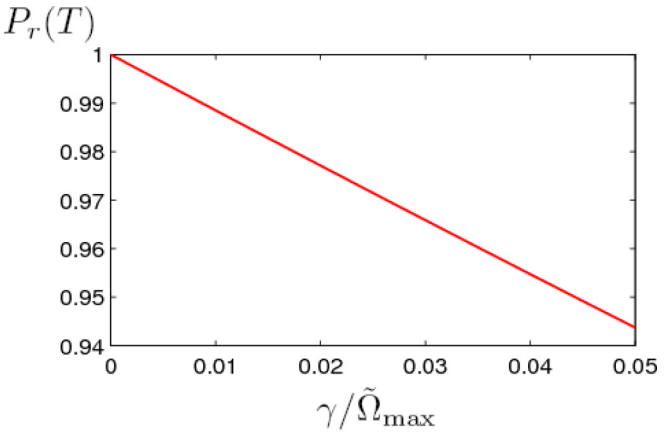

FIG. 8. Final population $P_r(T)$ of Rydberg state $|r\rangle$ versus $\gamma/\tilde{\Omega}_{\max}$.

2. *Off-resonant case*

Now, let us briefly discuss the population transfer $|g\rangle \to |r\rangle$ of the cascaded three-level Rydberg atom in the off-resonant case. We assume the detunings of transitions $|g\rangle \leftrightarrow |e\rangle$ and $|e\rangle \leftrightarrow |r\rangle$ are $\Delta_1(t)$ and $\Delta_3(t)$, respectively. According to Eq. (24), we have

$$\begin{aligned}\Delta_1(t) &= \delta_1(t) + \delta_3(t),\\ \Delta_3(t) &= \delta_3(t) - \delta_1(t) - \delta_2(t),\\ \delta_3(t) &= -\delta_2(t).\end{aligned} \tag{46}$$

When considering the boundary conditions

$$\begin{aligned}\dot{\theta}_5(0) = \dot{\theta}_5(T) = \pi/2,\\ \dot{\theta}_1(0) = \pi/2,\ \dot{\theta}_1(T) = 0,\end{aligned} \tag{47}$$

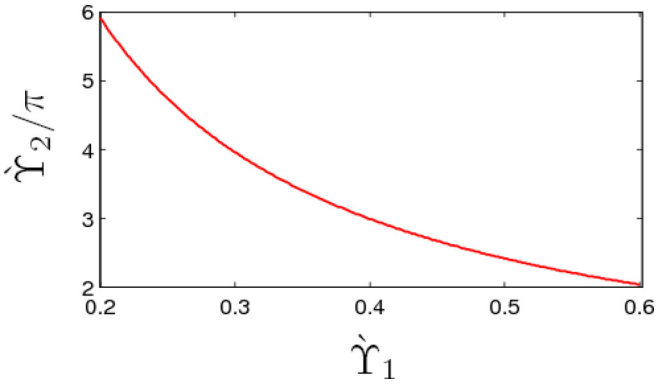

FIG. 9. The dependency relationship between $\dot{\Upsilon}_1$ and $\dot{\Upsilon}_2$.

the Rydberg atom will evolve along

$$\begin{aligned}|\dot{\psi}_3(t)\rangle &= \dot{U}_3(t)|g\rangle \\ &= e^{i\dot{\theta}_7}(\sin\dot{\theta}_1\sin\dot{\theta}_5|g\rangle + i\cos\dot{\theta}_5|e\rangle \\ &\quad + i\cos\dot{\theta}_1\sin\dot{\theta}_5|r\rangle),\end{aligned} \tag{48}$$

from $|g\rangle$ to $|r\rangle$ up to a global phase. Thus, according to Eqs. (27) and (47), we set

$$\begin{aligned}\dot{\theta}_5 &= \frac{\pi}{2} + \frac{\dot{\Upsilon}_1}{2}\left[1+\cos\left(\frac{2\pi t}{T}\right)\right], \\ \dot{\theta}_6 &= \frac{\dot{\Upsilon}_2}{\pi}\left[1-\cos\left(\frac{\pi t}{T}\right)\right], \\ \dot{\theta}_7 &= -\frac{\dot{\Upsilon}_3}{T}\sin\left(\frac{\pi t}{T}\right)\chi(t), \\ \dot{\theta}_8 &= \frac{\dot{\Upsilon}_3}{2T}\sin\left(\frac{\pi t}{T}\right)[\chi(t)+6\sin 2\dot{\theta}_1\sin^2\dot{\theta}_5],\end{aligned} \tag{49}$$

where $\dot{\Upsilon}_1$, $\dot{\Upsilon}_2$, and $\dot{\Upsilon}_3$ are three time-independent parameters controlling the maximal values of $\dot{\theta}_5$, $\dot{\theta}_6$, and $\dot{\theta}_{7(8)}$, respectively. Moreover, we should select $\dot{\Upsilon}_1$ and $\dot{\Upsilon}_2$ to satisfy

$$\dot{\theta}_1(T) = \frac{\pi}{2} + \int_0^T \dot{\theta}_6\cos\dot{\theta}_5 dt = 0. \tag{50}$$

By numerically calculating Eq. (50), we plot the dependency relationship between $\dot{\Upsilon}_1$ and $\dot{\Upsilon}_2$ in Fig. 9. As an example, we consider $\dot{\Upsilon}_1 = 0.4$ and $\dot{\Upsilon}_2 = 2.987\pi$ according to Fig. 9. Furthermore, as $\dot{\theta}_7$ influences only the global phase, we select $\dot{\Upsilon}_3 = 1.5$ as an example. With the parameters selected, we plot the populations of $|g\rangle$, $|e\rangle$, and $|r\rangle$ versus t/T in Fig. 10(a). In addition, $\dot{\Omega}_{1r}(t)$, $\dot{\Omega}_{1i}(t)$, and $\Delta_1(t)$ versus t/T are plotted in Fig. 10(b). Moreover, $\dot{\Omega}_{2r}(t)$, $\dot{\Omega}_{2i}(t)$, and $\Delta_3(t)$ versus t/T are plotted in Fig. 10(c). According to Fig. 10(a), we can achieve the population transfer $|g\rangle \to |r\rangle$ at $t = T$. This shows the calculation processes of the off-resonant case in Sec. III A are valid.

B. *N*-type four-level Rydberg atom

In this part, we briefly discuss the population transfer for an N-type four-level Rydberg atom. As shown in Fig. 11, we consider an N-type four-level Rydberg atom with a ground state $|g'\rangle$, an excited state $|e'\rangle$, a

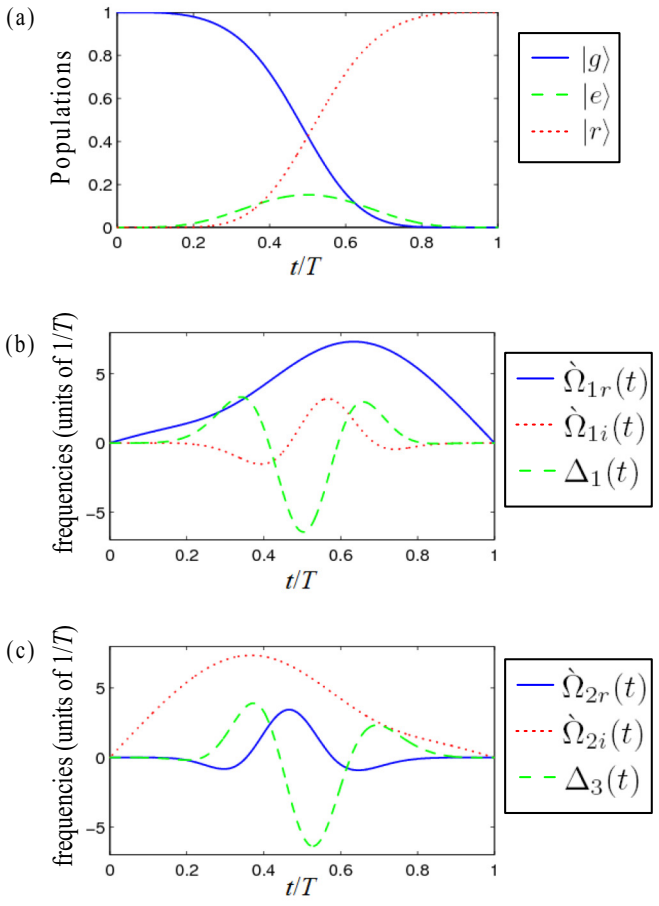

FIG. 10. (a) Populations of $|g\rangle$, $|e\rangle$, and $|r\rangle$ versus t/T. (b) $\dot{\Omega}_{1r}(t)$, $\dot{\Omega}_{1i}(t)$ and $\Delta_1(t)$ versus t/T. (c) $\dot{\Omega}_{2r}(t)$, $\dot{\Omega}_{2i}(t)$, and $\Delta_3(t)$.

metastable state $|m'\rangle$, and a Rydberg state $|r'\rangle$ [57]. In experiments, we can establish the atomic structure by using a ^{87}Rb atom with $|g'\rangle = |5s_{1/2}, F = 1, M_F = 0\rangle$, $|e'\rangle = |5p_{3/2}, F = 2, M_F = 0\rangle$, $|m'\rangle = |5s_{1/2}, F = 2, M_F = 0\rangle$, and $|r'\rangle = |97d_{5/2}, M_J = 5/2\rangle$ [57–59]. In the basis $\{|g'\rangle, |e'\rangle, |m'\rangle, |r'\rangle\}$, the Hamiltonian of the Rydberg atom can be described by the matrix shown in Eq. (31), with $\overline{\Omega}_1(t)$, $\overline{\Omega}_2(t)$, and $\overline{\Omega}_3(t)$ denoting the Rabi frequencies of laser pulses driving transitions $|g'\rangle \leftrightarrow |e'\rangle$, $|e'\rangle \leftrightarrow |m'\rangle$, and $|m'\rangle \leftrightarrow |r'\rangle$, respectively. Assume the Rydberg atom is initially in state $|g\rangle$ and the target is the Rydberg state $|r'\rangle$. According to Eq. (35),

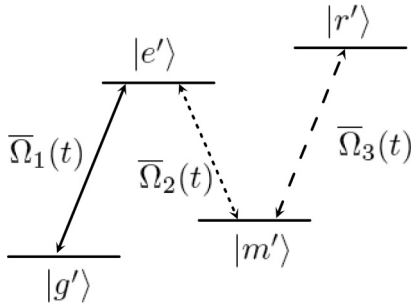

FIG. 11. The level configuration of an N-type four-level Rydberg atom.

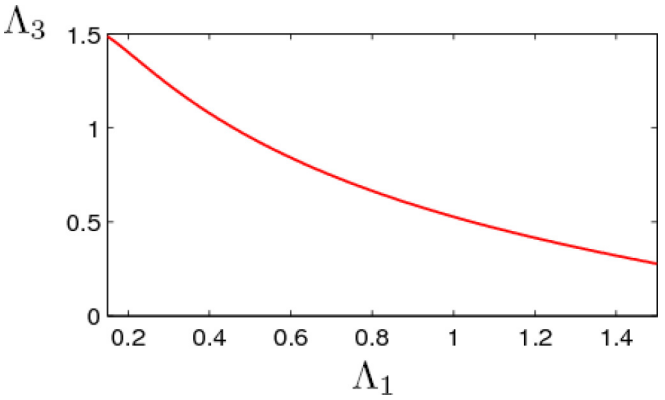

FIG. 12. The dependency relationship between Λ_1 and Λ_3.

the evolution of the Rydberg atom can be described by

$$\begin{aligned}|\psi_4(t)\rangle &= U_4(t)|g'\rangle \\ &= (\cos\overline{\theta}_1\cos\overline{\theta}_4\cos\overline{\theta}_5 - \sin\overline{\theta}_1\sin\overline{\theta}_3\sin\overline{\theta}_5)|g'\rangle \\ &\quad - i(\sin\overline{\theta}_1\cos\overline{\theta}_4\cos\overline{\theta}_5 + \cos\overline{\theta}_1\sin\overline{\theta}_3\sin\overline{\theta}_5)|e'\rangle \\ &\quad + (\cos\overline{\theta}_2\cos\overline{\theta}_3\sin\overline{\theta}_5 - \sin\overline{\theta}_2\sin\overline{\theta}_4\cos\overline{\theta}_5)|m'\rangle \\ &\quad - i(\cos\overline{\theta}_2\sin\overline{\theta}_4\cos\overline{\theta}_5 + \sin\overline{\theta}_2\cos\overline{\theta}_3\sin\overline{\theta}_5)|r'\rangle. \end{aligned} \tag{51}$$

Thus, the boundary conditions can be set as

$$\overline{\theta}_2(T) = \pi/2,\ \overline{\theta}_3(T) = 0,\ \overline{\theta}_5(T) = -\pi/2. \tag{52}$$

Therefore, parameters $\overline{\theta}_1(t)$, $\overline{\theta}_2(t)$, and $\overline{\theta}_3(t)$ can be chosen to be

$$\begin{aligned}\overline{\theta}_1(t) &= \Lambda_1 \sin\left(\frac{2\pi t}{T}\right)\sin\left(\frac{\pi t}{T}\right), \\ \overline{\theta}_2(t) &= \frac{\pi}{4}\left[1 - \cos\left(\frac{\pi t}{T}\right)\right], \\ \overline{\theta}_3(t) &= \Lambda_3 \sin^4\left(\frac{\pi t}{T}\right),\end{aligned} \tag{53}$$

where Λ_1 and Λ_3 are two time-independent parameters controlling the maximal values of $|\overline{\theta}_1|$ and $|\overline{\theta}_3|$, respectively. According to Eq. (34), Λ_1 and Λ_3 should be chosen to satisfy

$$\begin{aligned}\overline{\theta}_5(T) &= \int_0^T \frac{\dot{\overline{\theta}}_3(\cos\overline{\theta}_3\cos\overline{\theta}_4\tan\overline{\theta}_1 - \sin\overline{\theta}_3\sin\overline{\theta}_4\tan\overline{\theta}_2)}{\sin^2\overline{\theta}_3\sin^2\overline{\theta}_4 + \cos^2\overline{\theta}_3\cos^2\overline{\theta}_4}dt \\ &= -\pi/2.\end{aligned} \tag{54}$$

Given that Eq. (54) has a singularity when $\overline{\theta}_1 = \pi/2$, we consider Λ_1 in the range $[0,\pi/2]$. In addition, we set $\Lambda_3 \in [0,\pi/2]$ to avoid many oscillations of pulses. By numerically calculating the integral in Eq. (54), we can find the relation between Λ_1 and Λ_3, which is shown in Fig. 12. Here we consider parameters $\Lambda_1 = 0.4$ and $\Lambda_2 = 1.0782$. The populations of $|g'\rangle$, $|e'\rangle$, $|m'\rangle$, and $|r'\rangle$ versus t/T are plotted in Fig. 13(a). In addition, $\overline{\Omega}_1(t)$, $\overline{\Omega}_2(t)$, and $\overline{\Omega}_3(t)$ versus t/T are plotted in Fig. 13(b). As shown by Fig. 13, the population transfer succeeds at $t = T$, which confirms the results given in Sec. III B.

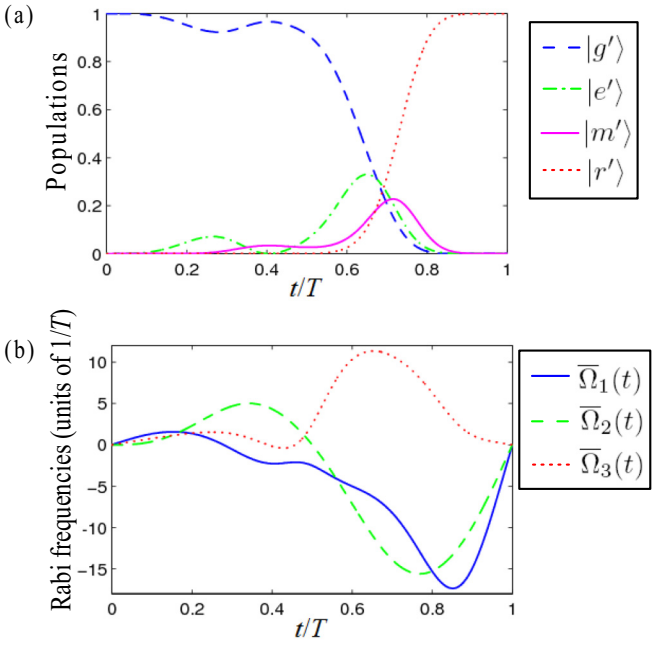

FIG. 13. (a) Populations of $|g'\rangle$, $|e'\rangle$, $|m'\rangle$, and $|r'\rangle$ versus t/T. (b) $\overline{\Omega}_1(t)$, $\overline{\Omega}_2(t)$, and $\overline{\Omega}_3(t)$ versus t/T.

V. CONCLUSION

In conclusion, we proposed a scheme for pulse design in multilevel systems. By analyzing the dynamic symmetry of a multilevel system in a Lie algebra, we gave a general formula to reverse construct a control Hamiltonian via a sequence of Lie transforms. Then, with that method, we studied the pulse design for three- and four-level systems. To show the feasibility of the scheme in a real physical system, as an example, we used the designed pulses to perform the population transfers of cascaded three-level and N-type four-level Rydberg atoms. Numerical simulations showed both of the population transfers can be achieved perfectly, which proved the validity of the scheme. Furthermore, we notice that the optimal control theory [11–18] provides many effective means to optimize the pulse shapes, which can help us make a good trade-off between energy cost and the robustness against the noise and decoherence. Thus, combined use of the optimal control theory and the current scheme to design pulses may be interesting and deserves further investigation. Since we discussed only the applications of the scheme in three- and four-level systems, generalizing the scheme to a more complex quantum system is also an interesting open question. Generally, the dynamics of a multilevel quantum system should be discussed in a Lie algebra with many generators when the system is very complex. But as long as the Hamiltonian of the system can still be described by generators of a Lie algebra, the scheme can still be applied to design pulses to drive the system. But there should be a positive correlation between the amount of calculation and the number of generators of the Lie algebra being investigated. More specifically, the number of independent parameters and constraint equations increases with the number of generators. Thus, studying a more complex multilevel system requires a more complex calculation when directly using the current scheme. To simplify or reduce calculations and make the

pulse design easy to realize in a complex system, a good choice may be combining the use of other approaches, such as quantum Zeno dynamics [60,61], perturbation theory [62,63], etc. Finally, although we discuss only the state-to-state transfer, the scheme can also be used to generate unitary propagators according to the unitary evolution operators shown in Eqs. (21), (29), and (35). Therefore, one may also apply the scheme to design pulses to implement quantum logic gates in a multilevel system.

ACKNOWLEDGMENTS

This work was supported by the National Natural Science Foundation of China under Grants No. 11575045, No. 11674060, and No. 11747011; the Major State Basic Research Development Program of China under Grant No. 2012CB921601; and the Natural Science Foundation of Fujian Province under Grant No. JAT160081.

APPENDIX A: THE DERIVATION OF RABI FREQUENCIES OF A THREE-LEVEL SYSTEM IN THE OFF-RESONANCE CASE

Generators $\grave{A}_J$ ($J = 1,2,\ldots,8$) shown in Sec. III A 2 can be written as

$$\grave{A}_1 = \begin{bmatrix} 0 & 0 & 1 \\ 0 & 0 & 0 \\ 1 & 0 & 0 \end{bmatrix},$$
$$\grave{A}_2 = \begin{bmatrix} 0 & 1 & 0 \\ 1 & 0 & 0 \\ 0 & 0 & 0 \end{bmatrix},$$
$$\grave{A}_3 = \begin{bmatrix} 0 & 0 & 0 \\ 0 & 0 & 1 \\ 0 & 1 & 0 \end{bmatrix},$$
$$\grave{A}_4 = \begin{bmatrix} 0 & 0 & -i \\ 0 & 0 & 0 \\ i & 0 & 0 \end{bmatrix},$$
$$\grave{A}_5 = \begin{bmatrix} 0 & -i & 0 \\ i & 0 & 0 \\ 0 & 0 & 0 \end{bmatrix},$$
$$\grave{A}_6 = \begin{bmatrix} 0 & 0 & 0 \\ 0 & 0 & i \\ 0 & -i & 0 \end{bmatrix},$$
$$\grave{A}_7 = \begin{bmatrix} 1 & 0 & 0 \\ 0 & 0 & 0 \\ 0 & 0 & -1 \end{bmatrix},$$
$$\grave{A}_8 = \begin{bmatrix} 0 & 0 & 0 \\ 0 & 1 & 0 \\ 0 & 0 & -1 \end{bmatrix}. \tag{A1}$$

The results of $-i[\grave{A}_J, \grave{A}_{J'}]$ are summarized in Table II. In the basis $\{\grave{A}_J | J = 1,2,\ldots,8\}$, the Lie transforms $\{\hat{\mathscr{L}}_J\}$ defined by $\{\grave{A}_J\}$ ($k = 1,2,3$) are eight 8×8 matrices, which can be derived in a way similar to the derivation of Eq. (14). Here we do not list the matrix forms of $\{\hat{\mathscr{L}}_J\}$ since they are very complex. In addition, we consider $\grave{\theta}_3 = \pi/2$ and $\grave{\theta}_4 = \pi/2 - \grave{\theta}_2$ to simplify the calculation. Then, by using Eq. (9), we can derive Eqs. (26) and (27).

TABLE II. The results of $-i[\grave{A}_J, \grave{A}_{J'}]$.

$\grave{A}_{J'}$ \ $\grave{A}_J$	$\grave{A}_1$	$\grave{A}_2$	$\grave{A}_3$	$\grave{A}_4$	$\grave{A}_5$	$\grave{A}_6$	$\grave{A}_7$	$\grave{A}_8$
$\grave{A}_1$	0	$-\grave{A}_6$	$-\grave{A}_5$	$-2\grave{A}_7$	$\grave{A}_3$	$\grave{A}_2$	$2\grave{A}_4$	$\grave{A}_4$
$\grave{A}_2$	$\grave{A}_6$	0	$-\grave{A}_4$	$\grave{A}_3$	$2(\grave{A}_8 - \grave{A}_7)$	$-\grave{A}_1$	$\grave{A}_5$	$-\grave{A}_5$
$\grave{A}_3$	$\grave{A}_5$	$\grave{A}_4$	0	$-\grave{A}_2$	$-\grave{A}_1$	$2\grave{A}_8$	$-\grave{A}_6$	$-2\grave{A}_6$
$\grave{A}_4$	$2\grave{A}_7$	$-\grave{A}_3$	$\grave{A}_2$	0	$-\grave{A}_6$	$\grave{A}_5$	$-2\grave{A}_1$	$-\grave{A}_1$
$\grave{A}_5$	$-\grave{A}_3$	$2(\grave{A}_7 - \grave{A}_8)$	$\grave{A}_1$	$\grave{A}_6$	0	$-\grave{A}_4$	$-\grave{A}_2$	$\grave{A}_2$
$\grave{A}_6$	$-\grave{A}_2$	$\grave{A}_1$	$-2\grave{A}_8$	$-\grave{A}_5$	$\grave{A}_4$	0	$\grave{A}_3$	$2\grave{A}_3$
$\grave{A}_7$	$-2\grave{A}_4$	$-\grave{A}_5$	$\grave{A}_6$	$2\grave{A}_1$	$\grave{A}_2$	$-\grave{A}_3$	0	0
$\grave{A}_8$	$-\grave{A}_4$	$\grave{A}_5$	$2\grave{A}_6$	$\grave{A}_1$	$-\grave{A}_2$	$-2\grave{A}_3$	0	0

APPENDIX B: THE DERIVATION OF RABI FREQUENCIES OF THE FOUR-LEVEL SYSTEM

Generators $\overline{A}_l$ ($l = 1,2,\cdots,6$) shown in Sec. III B can be written as

$$\overline{A}_1 = \begin{bmatrix} 0 & 1 & 0 & 0 \\ 1 & 0 & 0 & 0 \\ 0 & 0 & 0 & 0 \\ 0 & 0 & 0 & 0 \end{bmatrix},$$
$$\overline{A}_2 = \begin{bmatrix} 0 & 0 & 0 & 0 \\ 0 & 0 & 1 & 0 \\ 0 & 1 & 0 & 0 \\ 0 & 0 & 0 & 0 \end{bmatrix},$$
$$\overline{A}_3 = \begin{bmatrix} 0 & 0 & 0 & 0 \\ 0 & 0 & 0 & 0 \\ 0 & 0 & 0 & 1 \\ 0 & 0 & 1 & 0 \end{bmatrix},$$
$$\overline{A}_4 = \begin{bmatrix} 0 & 0 & -i & 0 \\ 0 & 0 & 0 & 0 \\ i & 0 & 0 & 0 \\ 0 & 0 & 0 & 0 \end{bmatrix},$$
$$\overline{A}_5 = \begin{bmatrix} 0 & 0 & 0 & 0 \\ 0 & 0 & 0 & -i \\ 0 & 0 & 0 & 0 \\ 0 & i & 0 & 0 \end{bmatrix},$$
$$\overline{A}_6 = \begin{bmatrix} 0 & 0 & 0 & 1 \\ 0 & 0 & 0 & 0 \\ 0 & 0 & 0 & 0 \\ 1 & 0 & 0 & 0 \end{bmatrix}. \tag{B1}$$

The results of $-i[\overline{A}_l, \overline{A}_{l'}]$ can be summarized in Table III.

TABLE III. The results of $-i[\overline{A}_l, \overline{A}_{l'}]$.

$\overline{A}_{l'}$ \ $\overline{A}_l$	$\overline{A}_1$	$\overline{A}_2$	$\overline{A}_3$	$\overline{A}_4$	$\overline{A}_5$	$\overline{A}_6$
$\overline{A}_1$	0	$-\overline{A}_4$	0	$\overline{A}_2$	$\overline{A}_6$	$-\overline{A}_5$
$\overline{A}_2$	$\overline{A}_4$	0	$-\overline{A}_5$	$-\overline{A}_1$	$\overline{A}_3$	0
$\overline{A}_3$	0	$\overline{A}_5$	0	$-\overline{A}_6$	$-\overline{A}_2$	$\overline{A}_4$
$\overline{A}_4$	$-\overline{A}_2$	$\overline{A}_1$	$\overline{A}_6$	0	0	$-\overline{A}_3$
$\overline{A}_5$	$-\overline{A}_6$	$-\overline{A}_3$	$\overline{A}_2$	0	0	$\overline{A}_1$
$\overline{A}_6$	$\overline{A}_5$	0	$-\overline{A}_4$	$\overline{A}_3$	$-\overline{A}_1$	0

Considering the commutation relations $[\overline{A}_1, \overline{A}_3] = 0$, $[\overline{A}_2, \overline{A}_6] = 0$, and $[\overline{A}_4, \overline{A}_5] = 0$, we rearrange the six operators as

$$\overline{B}_1 = \overline{A}_1,\ \overline{B}_2 = \overline{A}_3,\ \overline{B}_3 = \overline{A}_2,$$
$$\overline{B}_4 = \overline{A}_6,\ \overline{B}_5 = \overline{A}_4,\ \overline{B}_6 = \overline{A}_5 \tag{B2}$$

to simplify the calculation. In the basis $\{\overline{B}_l | l = 1,2,\ldots,6\}$, the matrices of the Lie transforms $\{\overline{\mathscr{L}}_l\}$ defined by $\{\overline{B}_l\}$ ($k = 1,2,3$) are

$$\overline{\mathscr{L}}_1 = \begin{bmatrix} 1 & 0 & 0 & 0 & 0 & 0 \\ 0 & 1 & 0 & 0 & 0 & 0 \\ 0 & 0 & \cos\overline{\theta}_1 & 0 & \sin\overline{\theta}_1 & 0 \\ 0 & 0 & 0 & \cos\overline{\theta}_1 & 0 & \sin\overline{\theta}_1 \\ 0 & 0 & -\sin\overline{\theta}_1 & 0 & \cos\overline{\theta}_1 & 0 \\ 0 & 0 & 0 & -\sin\overline{\theta}_1 & 0 & \cos\overline{\theta}_1 \end{bmatrix},$$

$$\overline{\mathscr{L}}_2 = \begin{bmatrix} 1 & 0 & 0 & 0 & 0 & 0 \\ 0 & 1 & 0 & 0 & 0 & 0 \\ 0 & 0 & \cos\overline{\theta}_2 & 0 & 0 & -\sin\overline{\theta}_2 \\ 0 & 0 & 0 & \cos\overline{\theta}_2 & -\sin\overline{\theta}_2 & 0 \\ 0 & 0 & 0 & \sin\overline{\theta}_2 & \cos\overline{\theta}_2 & 0 \\ 0 & 0 & \sin\overline{\theta}_2 & 0 & 0 & \cos\overline{\theta}_2 \end{bmatrix},$$

$$\overline{\mathscr{L}}_3 = \begin{bmatrix} \cos\overline{\theta}_3 & 0 & 0 & 0 & -\sin\overline{\theta}_3 & 0 \\ 0 & \cos\overline{\theta}_3 & 0 & 0 & 0 & \sin\overline{\theta}_3 \\ 0 & 0 & 1 & 0 & 0 & 0 \\ 0 & 0 & 0 & 1 & 0 & 0 \\ \sin\overline{\theta}_3 & 0 & 0 & 0 & \cos\overline{\theta}_3 & 0 \\ 0 & -\sin\overline{\theta}_3 & 0 & 0 & 0 & \cos\overline{\theta}_3 \end{bmatrix},$$

$$\overline{\mathscr{L}}_4 = \begin{bmatrix} \cos\overline{\theta}_4 & 0 & 0 & 0 & 0 & -\sin\overline{\theta}_4 \\ 0 & \cos\overline{\theta}_4 & 0 & 0 & \sin\overline{\theta}_4 & 0 \\ 0 & 0 & 1 & 0 & 0 & 0 \\ 0 & 0 & 0 & 1 & 0 & 0 \\ 0 & -\sin\overline{\theta}_4 & 0 & 0 & \cos\overline{\theta}_4 & 0 \\ \sin\overline{\theta}_4 & 0 & 0 & 0 & 0 & \cos\overline{\theta}_4 \end{bmatrix},$$

$$\overline{\mathscr{L}}_5 = \begin{bmatrix} \cos\overline{\theta}_5 & 0 & \sin\overline{\theta}_5 & 0 & 0 & 0 \\ 0 & \cos\overline{\theta}_5 & 0 & -\sin\overline{\theta}_5 & 0 & 0 \\ -\sin\overline{\theta}_5 & 0 & \cos\overline{\theta}_5 & 0 & 0 & 0 \\ 0 & \sin\overline{\theta}_5 & 0 & \cos\overline{\theta}_5 & 0 & 0 \\ 0 & 0 & 0 & 0 & 1 & 0 \\ 0 & 0 & 0 & 0 & 0 & 1 \end{bmatrix},$$

$$\overline{\mathscr{L}}_6 = \begin{bmatrix} \cos\overline{\theta}_6 & 0 & 0 & \sin\overline{\theta}_6 & 0 & 0 \\ 0 & \cos\overline{\theta}_6 & -\sin\overline{\theta}_6 & 0 & 0 & 0 \\ 0 & \sin\overline{\theta}_6 & \cos\overline{\theta}_6 & 0 & 0 & 0 \\ -\sin\overline{\theta}_6 & 0 & 0 & \cos\overline{\theta}_6 & 0 & 0 \\ 0 & 0 & 0 & 0 & 1 & 0 \\ 0 & 0 & 0 & 0 & 0 & 1 \end{bmatrix}. \tag{B3}$$

By using Eq. (9), we can derive Eq. (33) and the constraint equations

$$\dot{\overline{\theta}}_5(\cos\overline{\theta}_1\cos\overline{\theta}_2\cos\overline{\theta}_3\cos\overline{\theta}_4 - \sin\overline{\theta}_1\sin\overline{\theta}_2\sin\overline{\theta}_3\sin\overline{\theta}_4)$$
$$+\dot{\overline{\theta}}_6(\sin\overline{\theta}_1\sin\overline{\theta}_2\cos\overline{\theta}_3\cos\overline{\theta}_4 - \cos\overline{\theta}_1\cos\overline{\theta}_2\sin\overline{\theta}_3\sin\overline{\theta}_4)$$
$$+\dot{\overline{\theta}}_3\sin\overline{\theta}_1\cos\overline{\theta}_2 - \dot{\overline{\theta}}_4\cos\overline{\theta}_1\sin\overline{\theta}_2 = 0, \tag{B4}$$

$$\dot{\overline{\theta}}_5(\cos\overline{\theta}_1\sin\overline{\theta}_2\cos\overline{\theta}_3\cos\overline{\theta}_4 + \sin\overline{\theta}_1\cos\overline{\theta}_2\sin\overline{\theta}_3\sin\overline{\theta}_4)$$
$$-\dot{\overline{\theta}}_6(\sin\overline{\theta}_1\cos\overline{\theta}_2\cos\overline{\theta}_3\cos\overline{\theta}_4 + \cos\overline{\theta}_1\sin\overline{\theta}_2\sin\overline{\theta}_3\sin\overline{\theta}_4)$$
$$+\dot{\overline{\theta}}_3\sin\overline{\theta}_1\sin\overline{\theta}_2 + \dot{\overline{\theta}}_4\cos\overline{\theta}_1\cos\overline{\theta}_2 = 0, \tag{B5}$$

$$\dot{\overline{\theta}}_5(\cos\overline{\theta}_1\cos\overline{\theta}_2\sin\overline{\theta}_3\sin\overline{\theta}_4 - \sin\overline{\theta}_1\sin\overline{\theta}_2\cos\overline{\theta}_3\cos\overline{\theta}_4)$$
$$+\dot{\overline{\theta}}_6(\sin\overline{\theta}_1\sin\overline{\theta}_2\sin\overline{\theta}_3\sin\overline{\theta}_4 - \cos\overline{\theta}_1\cos\overline{\theta}_2\cos\overline{\theta}_3\cos\overline{\theta}_4)$$
$$+\dot{\overline{\theta}}_3\cos\overline{\theta}_1\sin\overline{\theta}_2 - \dot{\overline{\theta}}_4\sin\overline{\theta}_1\cos\overline{\theta}_2 = 0. \tag{B6}$$

Combining Eqs. (B4)–(B6), Eq. (34) can be derived.

[1] S. J. Glaser, U. Boscain, T. Calarco, C. P. Koch, W. Köckenberger, R. Kosloff, I. Kuprov, B. Luy, S. Schirmer, T. Schulte-Herbrüggen, D. Sugny, and F. K. Wilhelm, Eur. Phys. J. D **69**, 279 (2015).

[2] C. P. Yang, Phys. Rev. A **82**, 054303 (2010).

[3] A. Ruschhaupt, X. Chen, D. Alonso, and J. G. Muga, New J. Phys. **14**, 093040 (2012).

[4] G. T. Genov and N. V. Vitanov, Phys. Rev. Lett. **110**, 133002 (2013).

[5] B. T. Torosov and N. V. Vitanov, Phys. Rev. A **83**, 053420 (2011).

[6] S. B. Zheng, Phys. Rev. Lett. **95**, 080502 (2005).

[7] P. Král, I. Thanopulos, and M. Shapiro, Rev. Mod. Phys. **79**, 53 (2007).

[8] K. Bergmann, H. Theuer, and B. W. Shore, Rev. Mod. Phys. **70**, 1003 (1998).

[9] M. P. Fewell, B. W. Shore, and K. Bergmann, Aust. J. Phys. **50**, 281 (1997).

[10] N. V. Vitanov, T. Halfmann, B. W. Shore, and K. Bergmann, Annu. Rev. Phys. Chem. **52**, 763 (2001).

[11] D. Daems, A. Ruschhaupt, D. Sugny, and S. Guérin, Phys. Rev. Lett. **111**, 050404 (2013).

[12] D. Sugny and C. Kontz, Phys. Rev. A **77**, 063420 (2008).

[13] L. Van-Damme, D. Schraft, G. T. Genov, D. Sugny, T. Halfmann, and S. Guérin, Phys. Rev. A **96**, 022309 (2017).
[14] L. Van Damme, Q. Ansel, S. J. Glaser, and D. Sugny, Phys. Rev. A **95**, 063403 (2017).
[15] M. Lapert, G. Ferrini, and D. Sugny, Phys. Rev. A **85**, 023611 (2012).
[16] A. Garon, S. J. Glaser, and D. Sugny, Phys. Rev. A **88**, 043422 (2013).
[17] M. Lapert, E. Assémat, Y. Zhang, S. J. Glaser, and D. Sugny, Phys. Rev. A **87**, 043417 (2013).
[18] M. Lapert, Y. Zhang, M. Braun, S. J. Glaser, and D. Sugny, Phys. Rev. Lett. **104**, 083001 (2010).
[19] X. Chen, I. Lizuain, A. Ruschhaupt, D. Guéry-Odelin, and J. G. Muga, Phys. Rev. Lett. **105**, 123003 (2010).
[20] A. del Campo, Phys. Rev. Lett. **111**, 100502 (2013).
[21] A. del Campo, M. M. Rams, and W. H. Zurek, Phys. Rev. Lett. **109**, 115703 (2012).
[22] E. Torrontegui, S. Ibáñez, S. Martínez-Garaot, M. Modugno, A. del Campo, D. Guéry-Odelin, A. Ruschhaupt, X. Chen, and J. G. Muga, Adv. At. Mol. Opt. Phys. **62**, 117 (2013).
[23] J. G. Muga, X. Chen, A. Ruschhaupt, and D. Guéry-Odelin, J. Phys. B **42**, 241001 (2009).
[24] A. del Campo and M. G. Boshier, Sci. Rep. **2**, 648 (2012).
[25] H. Saberi, T. Opatrný, K. Mølmer, and A. del Campo, Phys. Rev. A **90**, 060301(R) (2014).
[26] S. Ibáñez, X. Chen, E. Torrontegui, J. G. Muga, and A. Ruschhaupt, Phys. Rev. Lett. **109**, 100403 (2012).
[27] S. Ibáñez, X. Chen, and J. G. Muga, Phys. Rev. A **87**, 043402 (2013).
[28] X. K. Song, Q. Ai, J. Qiu, and F. G. Deng, Phys. Rev. A **93**, 052324 (2016).
[29] E. Torrontegui, S. Ibáñez, X. Chen, A. Ruschhaupt, D. Guéry-Odelin, and J. G. Muga, Phys. Rev. A **83**, 013415 (2011).
[30] J. G. Muga, X. Chen, S. Ibáñez, I. Lizuain, and A. Ruschhaupt, J. Phys. B **43**, 085509 (2010).
[31] E. Torrontegui, X. Chen, M. Modugno, A. Ruschhaupt, D. Guéry-Odelin, and J. G. Muga, Phys. Rev. A **85**, 033605 (2012).
[32] X. Chen and J. G. Muga, Phys. Rev. A **82**, 053403 (2010).
[33] X. Chen, E. Torrontegui, D. Stefanatos, J. S. Li, and J. G. Muga, Phys. Rev. A **84**, 043415 (2011).
[34] A. del Campo, Eur. Phys. Lett. **96**, 60005 (2011).
[35] J. F. Schaff, X. L. Song, P. Vignolo, and G. Labeyrie, Phys. Rev. A **82**, 033430 (2010).
[36] X. Chen and J. G. Muga, Phys. Rev. A **86**, 033405 (2012).
[37] A. C. Santos, R. D. Silva, and M. S. Sarandy, Phys. Rev. A **93**, 012311 (2016).
[38] I. Hen, Phys. Rev. A **91**, 022309 (2015).
[39] S. Deffner, C. Jarzynski, and A. del Campo, Phys. Rev. X **4**, 021013 (2014).
[40] A. del Campo, Phys. Rev. A **84**, 031606(R) (2011).
[41] X. K. Song, H. Zhang, Q. Ai, J. Qiu, and F. G. Deng, New J. Phys. **18**, 023001 (2016).
[42] X. Chen, E. Torrontegui, and J. G. Muga, Phys. Rev. A **83**, 062116 (2011).
[43] X. Chen, A. Ruschhaupt, S. Schmidt, A. del Campo, D. Guéry-Odelin, and J. G. Muga, Phys. Rev. Lett. **104**, 063002 (2010).
[44] S. Ibáñez and J. G. Muga, Phys. Rev. A **89**, 033403 (2014).
[45] S. Martínez-Garaot, M. Palmero, D. Guéry-Odelin, and J. G. Muga, Phys. Rev. A **92**, 053406 (2015).
[46] S. Martínez-Garaot, M. Palmero, J. G. Muga, and D. Guéry-Odelin, Phys. Rev. A **94**, 063418 (2016).
[47] Y. H. Kang, Y. H. Chen, B. H. Huang, J. Song, and Y. Xia, Ann. Phys. (Berlin, Ger.) **529**, 1700004 (2017).
[48] Y. H. Kang, Z. C. Shi, B. H. Huang, J. Song, and Y. Xia, Ann. Phys. (Berlin, Ger.) **529**, 1700154 (2017).
[49] Y. C. Li, D. Martínez-Cercós, S. Martínez-Garaot, X. Chen, and J. G. Muga, Phys. Rev. A **97**, 013830 (2018).
[50] E. Torrontegui, S. Martínez-Garaot, and J. G. Muga, Phys. Rev. A **89**, 043408 (2014).
[51] U. Güngördü, Y. Wan, M. A. Fasihi, and M. Nakahara, Phys. Rev. A **86**, 062312 (2012).
[52] S. Martínez-Garaot, E. Torrontegui, X. Chen, and J. G. Muga, Phys. Rev. A **89**, 053408 (2014).
[53] M. M. Müller, M. Murphy, S. Montangero, T. Calarco, P. Grangier, and A. Browaeys, Phys. Rev. A **89**, 032334 (2014).
[54] T. Wilk, A. Gaëtan, C. Evellin, J. Wolters, Y. Miroshnychenko, P. Grangier, and A. Browaeys, Phys. Rev. Lett. **104**, 010502 (2010).
[55] D. Jaksch, J. I. Cirac, P. Zoller, S. L. Rolston, R. Côté, and M. D. Lukin, Phys. Rev. Lett. **85**, 2208 (2000).
[56] A. W. Carr and M. Saffman, Phys. Rev. Lett. **111**, 033607 (2013).
[57] X. Q. Shao, D. X. Li, Y. Q. Ji, J. H. Wu, and X. X. Yi, Phys. Rev. A **96**, 012328 (2017).
[58] L. Isenhower, E. Urban, X. L. Zhang, A. T. Gill, T. Henage, T. A. Johnson, T. G. Walker, and M. Saffman, Phys. Rev. Lett. **104**, 010503 (2010).
[59] X. L. Zhang, L. Isenhower, A. T. Gill, T. G. Walker, and M. Saffman, Phys. Rev. A **82**, 030306(R) (2010).
[60] P. Facchi and S. Pascazio, Phys. Rev. Lett. **89**, 080401 (2002).
[61] P. Facchi, V. Gorini, G. Marmo, S. Pascazio, and E. C. G. Sudarshan, Phys. Lett. A **275**, 12 (2000).
[62] D. F. V. James and J. Jerke, Can. J. Phys. **85**, 625 (2007).
[63] P. W. Milonni, D. F. V. James, and H. Fearn, Phys. Rev. A **52**, 1525 (1995).